



■ CARTILAGE

Interleukin-1 receptor antagonist protein (IL-1Ra) and miR-140 overexpression via pNNS-conjugated chitosan-mediated gene transfer enhances the repair of full-thickness cartilage defects in a rabbit model

**R. Zhao,
S. Wang,
L. Jia,
Q. Li,
J. Qiao,
X. Peng**

Weifang Medical
University, Weifang,
China

■ R. Zhao, PhD, Associate Professor,
■ L. Jia, BA, Postgraduate,
■ Q. Li, PhD, Lecturer,
■ J. Qiao, PhD, Lecturer,
■ X. Peng, MA, Associate Professor, Institute of Nanomedicine Technology, Department of Laboratory Medicine, Weifang Medical University, Weifang, China; Institutional Key Laboratory of Clinical Laboratory Diagnostics, 12th 5-Year project of Shandong Province, Weifang Medical University, Weifang, China; Key Discipline of Clinical Laboratory Medicine of Shandong Province, Affiliated Hospital of Weifang Medical University, Weifang, China.

■ S. Wang, BA, Supervisor Nurse, Department of Cardiovascular Medicine, Weifang Peoples Hospital, Weifang, China.

Correspondence should be sent to X. Peng; email: pxx74@sina.com

doi: 10.1302/2046-3758.83.BJR-2018-0222.R1

Bone Joint Res 2019;8:165–178.

Objectives

Previously, we reported the improved transfection efficiency of a plasmid DNA-chitosan (pDNA-CS) complex using a phosphorylatable nuclear localization signal-linked nucleic kinase substrate short peptide (pNNS) conjugated to chitosan (pNNS-CS). This study investigated the effects of pNNS-CS-mediated miR-140 and interleukin-1 receptor antagonist protein (IL-1Ra) gene transfection both in rabbit chondrocytes and a cartilage defect model.

Methods

The pBudCE4.1-miR-140, pBudCE4.1-IL-1Ra, and negative control pBudCE4.1 plasmids were constructed and combined with pNNS-CS to form pDNA/pNNS-CS complexes. These complexes were transfected into chondrocytes or injected into the knee joint cavity.

Results

High IL-1Ra and miR-140 expression levels were detected both *in vitro* and *in vivo*. *In vitro*, compared with the pBudCE4.1 group, the transgenic group presented with significantly increased chondrocyte proliferation and glycosaminoglycan (GAG) synthesis, as well as increased collagen type II alpha 1 chain (COL2A1), aggrecan (ACAN), and TIMP metalloproteinase inhibitor 1 (TIMP-1) levels. Nitric oxide (NO) synthesis was reduced, as were a disintegrin and metalloproteinase with thrombospondin type 1 motif 5 (ADAMTS-5) and matrix metalloproteinase (MMP)-13 levels. *In vivo*, the exogenous genes reduced the synovial fluid GAG and NO concentrations and the ADAMTS-5 and MMP-13 levels in cartilage. In contrast, COL2A1, ACAN, and TIMP-1 levels were increased, and the cartilage Mankin score was decreased in the transgenic group compared with the pBudCE4.1 group. Double gene combination produced greater efficacies than each single gene, both *in vitro* and *in vivo*.

Conclusion

This study suggests that pNNS-CS is a good candidate for treating cartilage defects via gene therapy, and that IL-1Ra in combination with miR-140 produces promising biological effects on cartilage defects.

Cite this article: *Bone Joint Res* 2019;8:165–178.

Keywords Chitosan, Gene therapy, Cartilage defect, MicroRNA-140, Interleukin-1 receptor antagonist protein, IL-1Ra, Rabbit

Article focus

- To determine the effects of miR-140 and interleukin-1 receptor antagonist protein (IL-1Ra) overexpression on full-thickness articular cartilage defects repairing in a rabbit model.
- To establish whether pNNS-conjugated chitosan (pNNS-CS) can mediate gene transfection both in rabbit chondrocytes and a cartilage defect model.

- To investigate the mechanism of IL-1Ra and miR-140's effects on experimental articular cartilage defects.

Key messages

- IL-1Ra and miR-140 gene combination produced synergistic effects not only for promoting cartilage proliferation, but also for inhibiting the inflammatory response and cartilage degradation.

- pNNS-CS can improve transfection efficiency in chondrocytes.
- Collagen type II alpha 1 chain (COL2A1), aggrecan (ACAN), and TIMP metalloproteinase inhibitor 1 (TIMP-1) expression was increased in transgenic groups both *in vitro* and *in vivo*, whereas a disintegrin and metalloproteinase with thrombospondin type 1 motif 5 (ADAMTS-5) and matrix metalloproteinase (MMP)-13 expression was reduced.

Strengths and limitations

- Intra-articular injection of IL-1Ra and miR-140 gene enhances the repair of full-thickness cartilage defects in a rabbit model.
- The beneficial effect of intra-articular IL-1Ra and miR-140 gene may be due to the inhibition of the inflammatory response and cartilage degradation.
- pNNS-CS could be a good candidate for treating cartilage defects via gene therapy.

Introduction

Articular cartilage is avascular and has a poor healing capacity.¹ A method that induces the proper repair of injured cartilage is needed. Currently, gene therapy has attracted more attention and has become a popular research topic.¹⁻⁵ Choosing the gene delivery method is very important for gene therapy, and many studies have been undertaken to develop safe and efficient gene delivery methods.²⁻⁷ Chitosan (CS), a polycationic non-viral gene carrier, has been studied by many researchers. The effect of CS nanoparticles carrying small interfering RNA (siRNA), microRNA (miRNA), or therapeutic genes on gene delivery has been studied both *in vitro* and *in vivo*.⁶⁻¹¹ However, the transfection efficiency of CS is low under physiological conditions. Many researchers, including the authors of this study, have tried to improve CS transfection efficiency through chemical structure modifications.^{6,7,9,11-13} In our previous study, we confirmed that pNNS conjugated to CS (pNNS-CS) improved the transfection efficiency of plasmid DNA (pDNA) in C2C12 myoblast cells.¹³ Therefore, we proposed the use of pNNS-CS as a gene carrier in gene therapy for the treatment of cartilage defects. However, the structure of C2C12 cells is significantly different from that of chondrocytes, and previously, we studied the transfection efficiency of pNNS-CS *in vitro* only. Many problems still need to be resolved, such as how to ensure the transfection efficiency of pNNS-CS in chondrocytes *in vivo*, whether intra-articular injections affect the pDNA/pNNS-CS complex stability, and whether pNNS-CS can become an efficient and reliable carrier for cartilage defect gene therapy. Therefore, this study attempts to use pNNS-CS as a carrier to transport exogenous genes into chondrocytes both *in vitro* and *in vivo*, thereby improving exogenous gene transfection efficiency and expression.

Articular cartilage regeneration involves many chondrogenic factors. Therefore, therapy with multiple recombinant genes may improve functional repair, and many studies have combined multiple genes to treat cartilage defects.^{5,10,14,15} Several cytokines play important roles in the metabolism of normal cartilage. Because of the chondroregenerative effects of cytokines, many genes coding for insulin-like growth factor I (IGF-I),^{1-3,10,11,14} transforming growth factor- β (TGF- β),^{5,14,15} transcription factor SOX9,^{1,5} and interleukin-1 receptor antagonist protein (IL-1Ra)^{10,15} have been transferred into chondrocytes both *in vitro* and *in vivo*. The results have demonstrated that the effects of combined gene transfer are superior to therapy with a single gene.^{4,10,14,15} IL-1Ra can block the adverse effects of IL-1 in OA by binding the IL-1 receptor and inhibiting articular cartilage extracellular matrix (ECM) degradation.¹⁶ miRNAs are a class of non-coding small RNAs.¹⁷ Many analyses have revealed that miRNAs are significantly dysregulated.¹⁸⁻²⁰ Many miRNAs play important roles in cartilage functional repair,²¹⁻²³ especially cartilage-specific miR-140.²²⁻²⁵ A study has shown that IL-1Ra protein treatment administered by intra-articular injections following a cartilage impact injury increased miR-140 expression in cartilage and prevented the degradation of cartilage ECM.²⁶ Therefore, in this study, we chose IL-1Ra and miR-140 as the therapeutic genes for treating cartilage defects.

In this study, we sought to determine whether pNNS-CS can carry IL-1Ra and miR-140 genes into chondrocytes and promote efficient expression. The effects of the exogenous genes were investigated both in cultured chondrocytes and in a cartilage defect animal model. The efficacy of the combinatorial IL-1Ra and miR-140 gene delivery was also explored.

Materials and Methods

Reagents and animals. CS was purchased from Sigma-Aldrich (St. Louis, Missouri). Dulbecco's Modified Eagle Medium (DMEM)/F12 medium, human IL-1RA enzyme-linked immunosorbent assay (ELISA) kits, and Annexin V-FITC apoptosis detection kits were purchased from Thermo Fisher (Shanghai, China). IL-1 β was purchased from PeproTech (Rocky Hill, New Jersey). Radioimmunoprecipitation assay (RIPA), phenylmethylsulfonyl fluoride (PMSF), and MTT were purchased from Solarbio Life Sciences (Beijing, China). We also purchased the following kits: a rabbit glycosaminoglycan (GAG) ELISA kit (Nanjing Sen Beijia Biotechnology, Nanjing, China); a nitrate reductase kit for nitric oxide (NO) detection (Nanjing JianCheng Bioengineering Institute, Nanjing, China); a SYBR Premix Ex Taq II, RNAiso Plus, Mir-X miRNA First-Strand Synthesis kit (Takara, Dalian, China); and a PrimeScript RT reagent kit (Takara). The KOD-Plus-Ver polymerase was purchased from TOYOBO (Tokyo, Japan), while the aggrecan (ACAN), collagen type

II alpha 1 chain (COL2A1), TIMP metalloproteinase inhibitor 1 (TIMP-1), a disintegrin and metalloproteinase with thrombospondin type 1 motif 5 (ADAMTS-5), and matrix metalloproteinase (MMP)-13 antibodies were purchased from Bioss (Beijing, China). New Zealand white rabbits were purchased from Jinan Jinfeng Experimental Animal Limited by Share Ltd. (Shandong, China). The protocols in this study that involved animals were approved by the Institutional Animal Care and Use Committee of Weifang Medical University.

pBudCE4.1 vector construction. The pBudCE4.1-IL-1Ra vector was previously constructed and reserved by our team.¹⁰ The human mature miR-140 sequence and its precursor pre-miR-140 were retrieved from the Ensembl (<http://asia.ensembl.org/index>) and NCBI (<https://www.ncbi.nlm.nih.gov/gene/>) databases, and their genomic position was localized and then flanked at both ends to obtain a sequence of approximately 210 bp (pri-miR-140, miR-140). miR-140 was amplified from human genomic DNA using the KOD-Plus-Ver polymerase. The forward primer 5'-CCCAAGCTTTTCCGTGGTGACCTCTCT-3' contained the *Hind*III restriction endonuclease site, and the reverse primer 5'-CgCGGATCCTGCTGGGCTGTTTGTGGCTG-3' contained a *Bam*HI site. The *Hind*III-*Bam*HI PCR product fragments were subcloned into the pBudCE4.1 plasmid at the corresponding sites. The pBudCE4.1-miR-140 expression plasmids were confirmed via sequence analysis. A random unrelated sequence was subcloned into the pBudCE4.1 plasmid to serve as a negative control (pBudCE4.1).

Preparation of pDNA/pNNS-CS complexes. pNNS was conjugated to CS to form pNNS-CS complexes as previously described.¹³ The pBudCE4.1-IL-1Ra, pBudCE4.1-miR-140, and pBudCE4.1 plasmids were mixed with pNNS-CS in weight ratios of 1:0.25, 1:0.5, 1:1, 1:1.5, 1:2, or 1:2.5 to form the pDNA/pNNS-CS complexes (pBudCE4.1-miR-140/pNNS-CS, pBudCE4.1-IL-1Ra/pNNS-CS, and pBudCE4.1/pNNS-CS), as previously described.¹⁰ Complex formation was detected by gel retardation assays. In the following experiments, the pDNA/pNNS-CS complexes were prepared at a pDNA:pNNS-CS weight ratio of 1:2. The enhanced green fluorescent protein (EGFP) reporter gene plasmid pEGFP-C1 was respectively mixed with pNNS-CS or CS at a weight ratio of 1:2 to form pEGFP/pNNS-CS and pEGFP/CS complexes. The transfection efficiency was determined by observing green fluorescent protein (GFP)-positive cells under a fluorescence microscope.

In vitro: chondrocyte isolation and culture transfection. Articular chondrocytes were isolated from one-week-old rabbits and cultured as described previously.¹⁰ Second-generation chondrocytes were used for the following experiments. The chondrocytes were divided into five groups: 1) the non-transfected group (control group); 2) the group transfected with pBudCE4.1/pNNS-CS, called the negative control group (pBudCE4.1);

3) the pBudCE4.1-IL-1Ra/pNNS-CS-transfected group (pBudCE4.1-IL-1Ra); 4) the pBudCE4.1-miR-140/pNNS-CS-transfected group (pBudCE4.1-miR-140); and 5) the pBudCE4.1-IL-1Ra+pBudCE4.1-miR-140/pNNS-CS-transfected group (pBudCE4.1-IL-1Ra+miR-140).

Chondrocytes were seeded at a density of 1×10^6 cells/ml and 5×10^4 cells/ml on six-well and 96-well microplates in complete DMEM/F12 supplemented with 10% foetal bovine serum (FBS) in a humidified incubator containing 5% CO₂ at 37°C. When the cells had grown to 50% confluence, the pDNA/pNNS-CS complexes were added to the six-well and 96-well microplates to achieve DNA concentrations of 4 µg/well and 0.25 µg/well. At 24 hours after transfection, the cells were treated with 10 ng/ml IL-1β to motivate delivery of IL-1Ra.²⁷

In vitro: detection of transgene expression. The above chondrocytes, seeded in six-well plates, were subjected to the following experiments after 72 hours of transfection. Cell supernatants were collected and analyzed by ELISA kits according to the manufacturer's instructions to determine the IL-1Ra concentration. Each sample was examined in triplicate. Total RNA from the chondrocytes was extracted using RNAiso Plus. Total RNA (2 µg) was reverse transcribed into total complementary DNA (cDNA) in a 10 µl reaction mixture using a Mir-X miRNA First-Strand Synthesis kit according to the manufacturer's protocol. The miR-140 expression levels were detected via real-time fluorescent quantitative polymerase chain reaction (RT-qPCR) in an iQ5 instrument (Bio-Rad; Hercules, California); the forward primer sequence was 5'-CGCGCCAGTGGTTTTACCTT-3', and the reverse primer and U6 primer were from the reverse transcription kit. Each RT-qPCR assay was run with triplicate technical samples. The raw miR-140 CT values were calibrated to that of the U6 reference gene, and the miR-140 expression of each sample was normalized. The $\Delta\Delta$ CT method was used to calculate miR-140 expression.

In vitro: chondrocyte proliferation. Cell proliferation was detected using a standard MTT method. Chondrocytes were seeded into 96-well plates and transfected as described above. At 72 hours after the transfection, MTT solution (15 µl; 5 mg/ml) was added to each well, and the plate was maintained at 37°C for four hours. The formazan crystals were dissolved in dimethylsulfoxide (150 µl/well), the absorption at 570 nm was measured using a microplate reader (Bio-Rad), and the background absorbance at 630 nm was subtracted. Each group experiment was repeated six times.

In vitro: GAG and NO concentrations in cell supernatants. At 72 hours after transfection, cell supernatants were collected and analyzed by ELISA and nitrate reductase kits according to the manufacturer's instructions to determine the GAG and NO concentrations, respectively.

In vitro: RT-qPCR analysis of COL2A1, ACAN, TIMP-1, ADAMTS-5, and MMP-13 levels. At 72 hours after transfection, the total RNA of chondrocytes seeded in six-well

Table I. Primers for each gene

Gene name	Gene symbol	Accession number	Amplicon length (bp)	Primer sequence
β -2-microglobulin dehydrogenase	B2M	XM_002717921.1	157	Forward: AACGTGGAACAGTCAGACC Reverse: AGTAATCTCGATCCCATTTTC
Collagen type II alpha 1 chain	COL2A1	NM_001195671.1	172	Forward: ATGGCGGCTTCCACTTCAG Reverse: CGGTGGCTTCATCCAGGTAG
Aggrecan	ACAN	XM_008251722.2	171	Forward: AGAACAGCGCCATCATTGC Reverse: CTCACGCCAGGGAACATCATC
A disintegrin and metalloproteinase with thrombospondin motifs 5	ADAMTS-5	AY382879.1	151	Forward: TGTCCAATTTCTGTGAGCC Reverse: TGTTACCAGAGAGGATTATG
Matrix metalloproteinase 13	MMP-13	NM_001082037.1	167	Forward: TGATGATGATGAAACTTGG Reverse: CATCAGGAAGCATAAAGTG
TIMP metalloproteinase inhibitor 1	TIMP-1	XM_008272340.2	151	Forward: ATGGAAAGTGTCTGCGGGTAC Reverse: AGCCGGAACGTTGAGAGAAG

plates was extracted using RNAiso Plus. The mRNA (2 μ g) was reverse transcribed into total cDNA using a PrimeScript RT reagent kit. COL2A1, ACAN, TIMP-1, ADAMTS-5, and MMP-13 expression levels were evaluated by RT-qPCR, using the β -2-microglobulin (B2M) gene as a reference gene.²⁸ The primers for each gene are shown in Table I. Each qPCR assay was run with triplicate technical samples. The CT values of all genes from the different samples were calibrated to B2M expression, the mRNA of each sample was normalized, and the $2^{-\Delta\Delta CT}$ values were used to calculate gene expression.

In vitro: Western blot analysis. Whole transfected chondrocyte lysates were prepared using lysis buffer (RIPA and 10 mM PMSF). These lysates were quantified by the bicinchoninic acid protein assay and separated by 8% SDS-polyacrylamide gel electrophoresis. Proteins were transferred from the gels to polyvinylidene difluoride (PVDF) membranes and immunoblotted with COL2A1 (1:200), ACAN (1:200), TIMP-1 (1:200), ADAMTS-5 (1:200), and MMP-13 (1:200) primary antibodies according to standard immunoblotting protocols. The anti-glyceraldehyde 3-phosphate dehydrogenase (GAPDH) antibody was used for the loading control. Proteins were visualized using enhanced chemiluminescence Western blot detection reagents, and pictures were captured using the ChemiDoc XRS+ System (Bio-Rad).

In vivo: animals and experimental cartilage defects. A total of 30 male rabbits (2.0 kg to 2.5 kg) were randomly divided into five groups with six rabbits each. After general anaesthesia, the first group had the knee joint cavity opened and sutured only (sham group). Groups 2 to 5 underwent gene delivery and 4 mm diameter, 3 mm deep artificial knee cartilage full-thickness defects were induced in the patellar groove of the femur, as previously described.²⁸ Intramuscular penicillin (400 000 U) injections and skin wound disinfection were performed for five days after surgery.

Seven days after the surgery, isotonic saline and the pDNA/pNNS-CS complexes were injected into the knee joint cavities of groups 1 to 5. These injections were administered twice a week for seven weeks. The amount

of pDNA in each intervention group was 15 μ g (each time), and the pDNA/ pNNS-CS complexes were dissolved in saline to adjust the volume to 0.2 ml. Eight weeks after surgery, the rabbits were sacrificed under general anaesthesia. The knee joint cavity was washed using isotonic saline through the patellar tendon. After centrifugation, the synovial fluid washes were used to analyze the IL-1Ra, GAG, and NO concentrations. Total RNA was extracted from one half of the cartilage defective area of each group and used for RT-qPCR (n = 6). The remaining half of the cartilage defective area from each group was subjected to histological evaluation (n = 6).

In vivo: IL-1Ra, GAG, and NO concentrations in the synovial fluid. The exogenous IL-1Ra, GAG, and NO concentrations in the synovial fluid were detected as described in the above *in vitro* study.

In vivo: RT-qPCR analysis of miR-140, COL2A1, ACAN, TIMP-1, ADAMTS-5, and MMP-13 expression. Total RNA was extracted from fresh cartilage tissue with RNAiso Plus. Total RNA was reverse transcribed into cDNA using a Mir-X miRNA First-Strand Synthesis kit and PrimeScript RT reagent kit. The miR-140, COL2A1, ACAN, TIMP-1, ADAMTS-5, and MMP-13 expression levels were detected via RT-qPCR as described in the above *in vitro* study.

In vivo: histological assay of articular cartilage injury and repair. Following the dissection, one half of the cartilage defective area from each group, including some hard bone tissue and surrounding cartilage, were quickly removed and fixed in 10% buffered formalin for 24 hours. The specimens were then decalcified in 10% ethylenediaminetetraacetic acid (EDTA) solution and embedded in paraffin. Next, 4 μ m sagittal sections of the defect area were cut and stained with haematoxylin and eosin (H&E), and safranin O/fast green staining and immunohistochemistry were conducted according to a standard protocol. The articular cartilage tissue structure was observed with an optical microscope (Olympus, Tokyo, Japan), and cartilage damage severity was scored according to the Mankin scale.²⁹

Statistical analysis. All data measurements are expressed as means and standard deviations, and were analyzed

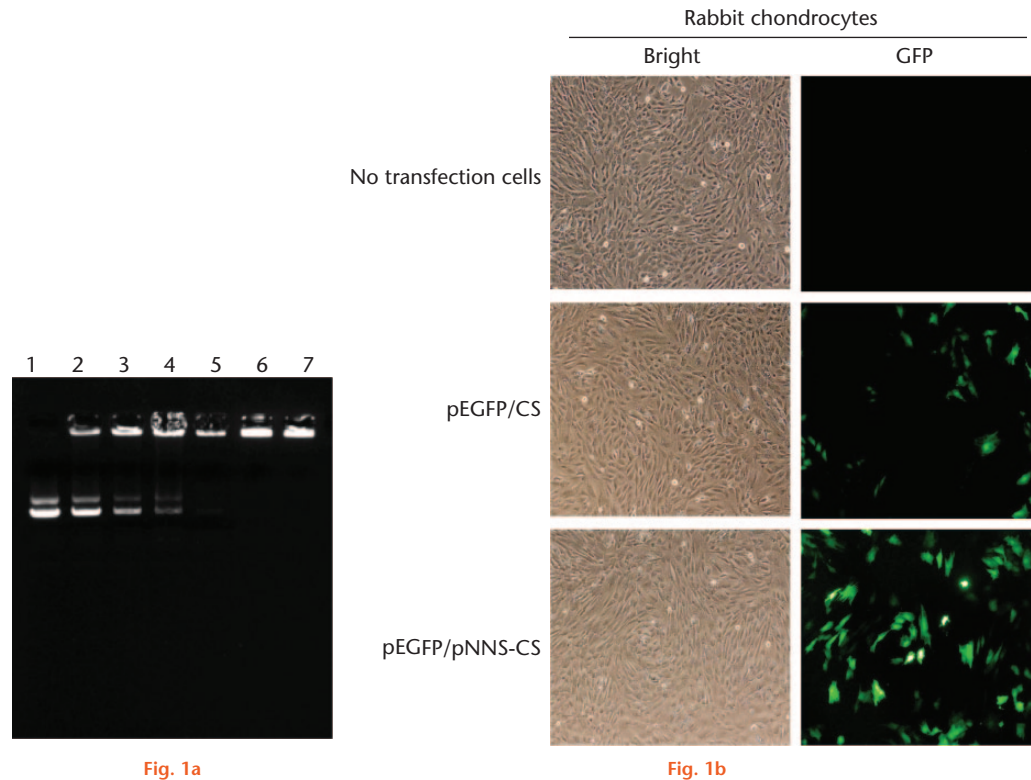


Fig. 1a

Fig. 1b

Electrophoresis and transfection efficiency of the plasmid DNA (pDNA)/pNNS conjugated to chitosan (pNNS-CS) complex. a) Agarose gel electrophoresis of the pDNA/pNNS-CS complexes. Lane 1: free pDNA; lanes 2 to 7: pDNA/pNNS-CS (w/w) = 1:0.25; 1:0.5; 1:1; 1:1.5; 1:2; 1:2.5. When pDNA/pNNS-CS reached a weight ratio of 1:2, these complexes lost their mobility in the gel. b) The transfection efficiency of pDNA/pNNS-CS and pDNA/CS complexes in rabbit chondrocytes. Chondrocytes were transfected with pEGFP/pNNS-CS and pEGFP/CS for 72 hours; then green fluorescent protein (GFP) was observed under a fluorescence microscope (100 \times).

with SPSS 17.0 software (IBM Corp., Armonk, New York). Single-factor analysis of variance was used for multi-group comparisons. Each result was compared using the Student–Newman–Keuls test. Statistical significance was defined by a value of $p < 0.05$.

Results

Agarose gel electrophoresis and transfection efficiency of pDNA/pNNS-CS complexes. When the pDNA:pNNS-CS ratio was at or above 1:2, the pDNA/pNNS-CS complexes lost their mobility in the gel (Fig. 1a). Fluorescence microscopy analysis revealed that chondrocytes were transfected with pEGFP-C1, since more than 50% of the cells were GFP-positive at 72 hours post-transfection, and pNNS conjugation increased EGFP gene expression (Fig. 1b).

In vitro: effects of miR-140 and IL-1Ra on chondrocyte proliferation. The miR-140 expression levels in chondrocytes were similarly increased in the pBudCE4.1-miR-140 and pBudCE4.1-IL-1Ra+miR-140 groups compared with the other groups ($p < 0.01$). No significant difference was observed among the pBudCE4.1-IL-1Ra versus pBudCE4.1 group ($p = 0.861$), pBudCE4.1-IL-1Ra versus control group ($p = 0.531$), or pBudCE4.1 versus control group ($p = 0.691$) (Fig. 2a). The IL-1Ra expression levels in the cell supernatants were similarly increased in

the pBudCE4.1-IL-1Ra and pBudCE4.1-IL-1Ra+miR-140 groups compared with the other groups ($p < 0.01$). No significant differences were observed among the pBudCE4.1-miR-140 versus pBudCE4.1 group ($p = 0.648$), pBudCE4.1-miR-140 versus control group ($p = 0.688$), or pBudCE4.1 versus control group ($p = 0.955$) (Fig. 2b). Chondrocyte proliferation significantly increased in the pBudCE4.1-IL-1Ra+miR-140 group, followed by the pBudCE4.1-miR-140 group and the pBudCE4.1-IL-1Ra group, compared with the control group ($p < 0.01$). There was a significant difference in chondrocyte proliferation between the pBudCE4.1-miR-140 group and the pBudCE4.1-IL-1Ra group ($p = 0.048$), and there was no significant difference between the pBudCE4.1 group and control groups ($p = 0.759$) (Fig. 2c).

In vitro: GAG and NO concentrations in cell supernatants. The GAG levels were gradually increased in the pBudCE4.1, pBudCE4.1-miR-140, pBudCE4.1-IL-1Ra, and pBudCE4.1-IL-1Ra+ miR-140 groups compared with the control group ($p = 0.027$, $p < 0.001$, $p < 0.001$, and $p < 0.001$, respectively) (Fig. 3a). The NO levels were lowest in the pBudCE4.1-IL-1Ra+miR-140 group, followed by the pBudCE4.1-IL-1Ra and pBudCE4.1-miR-140 groups, compared with the control group ($p < 0.001$, $p < 0.001$, and $p = 0.001$, respectively). NO levels were

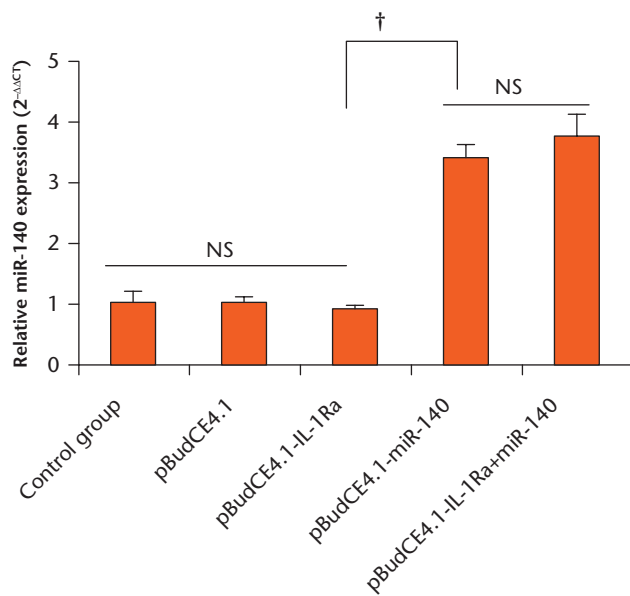


Fig. 2a

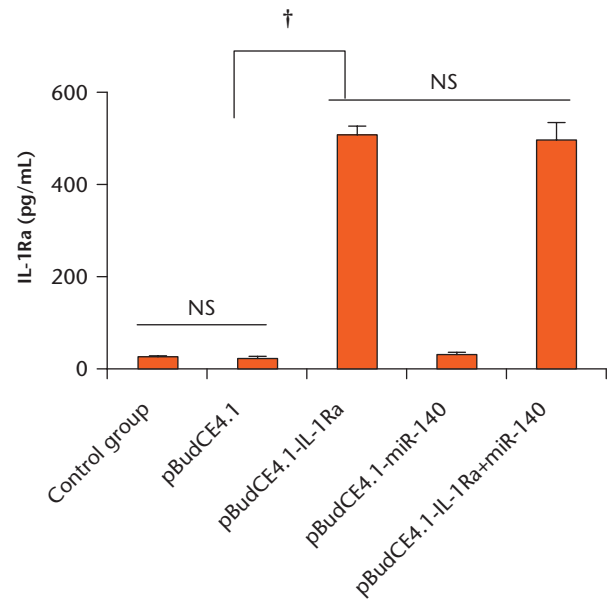


Fig. 2b

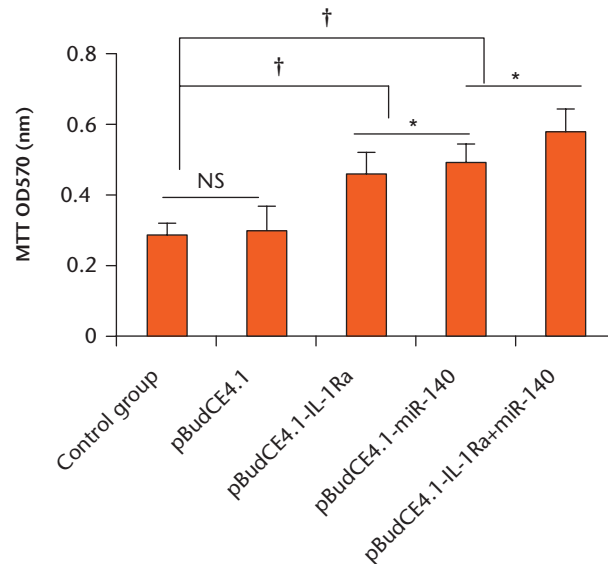


Fig. 2c

Graphs showing the effect on rabbit chondrocyte proliferation of a) interleukin-1 receptor antagonist protein (IL-1Ra) and b) miR-140 expression. The relative miR-140 expression level in different groups was determined by real-time fluorescent quantitative polymerase chain reaction (RT-qPCR). miR-140 gene expression in each group was normalized to the U6 expression level. The IL-1Ra concentration in the cell supernatant was analyzed by enzyme-linked immunosorbent assay (ELISA). c) Graph showing rabbit chondrocyte cell proliferation *in vitro* by the MTT method. The data are shown as mean values and standard deviations. * $p < 0.05$; † $p < 0.01$; NS, not significant.

not significantly different between the pBudCE4.1 and control groups ($p = 0.518$) (Fig. 3b).

***In vitro*: RT-qPCR and western blot quantification of COL2A1, ACAN, TIMP-1, ADAMTS-5, and MMP-13 expression in chondrocytes.** COL2A1, ACAN, and TIMP-1 expression levels were significantly increased, and ADAMTS-5 and MMP-13 expression levels were decreased significantly in the pBudCE4.1-IL-1Ra+miR-140 group, followed by the pBudCE4.1-miR-140 and pBudCE4.1-IL-1Ra groups, compared with the control group (all $p < 0.05$).

Moreover, compared with the pBudCE4.1-IL-1Ra group, the pBudCE4.1-miR-140 group presented with significantly higher COL2A1, ACAN, and MMP-13 expression levels and lower ADAMTS-5 and TIMP-1 levels ($p < 0.05$). However, no significant difference in the expression of these genes was detected between the control and pBudCE4.1 groups (all $p > 0.05$) (Figs 4a to 4e). Western blotting results also showed that the expression of these genes (Fig. 4f) was consistent with the mRNAs findings.

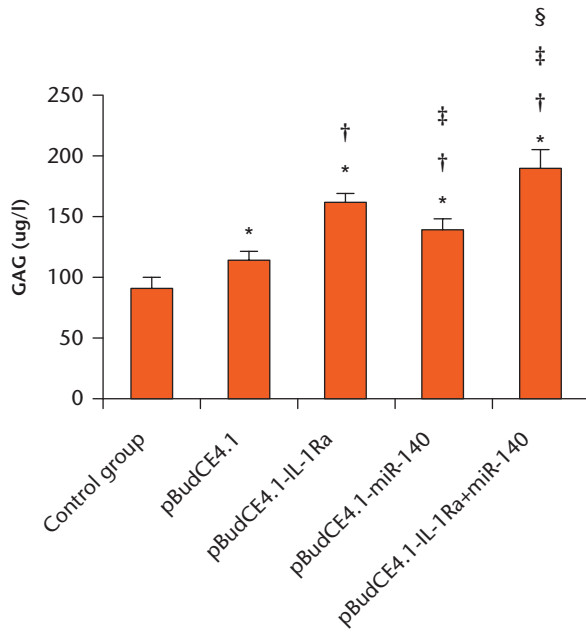


Fig. 3a

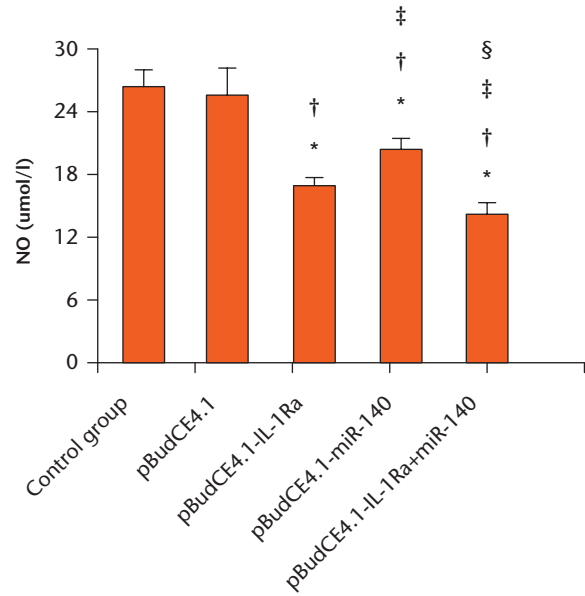


Fig. 3b

Graphs showing a) glycosaminoglycan (GAG) and b) nitric oxide (NO) concentrations in the cell supernatant. The GAG concentration in the cell supernatant was measured by enzyme-linked immunosorbent assay (ELISA). The NO levels in the cell supernatant were measured by a nitrate reductase assay. The data are shown as mean values and standard deviations. * $p < 0.05$ versus control group; † $p < 0.05$ versus pBudCE4.1; ‡ $p < 0.05$ versus pBudCE4.1-IL-1Ra; § $p < 0.05$ versus pBudCE4.1-miR-140.

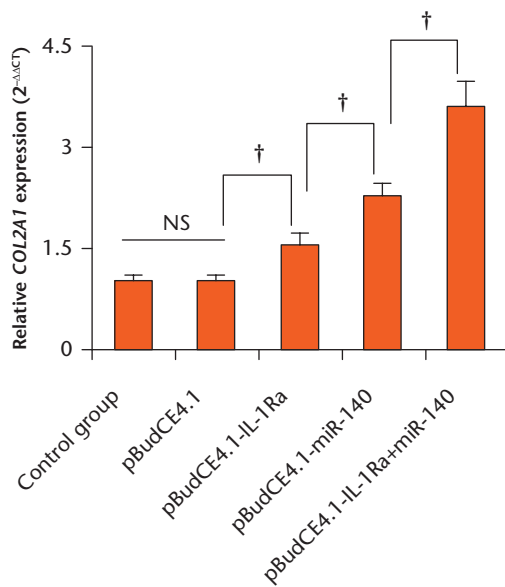


Fig. 4a

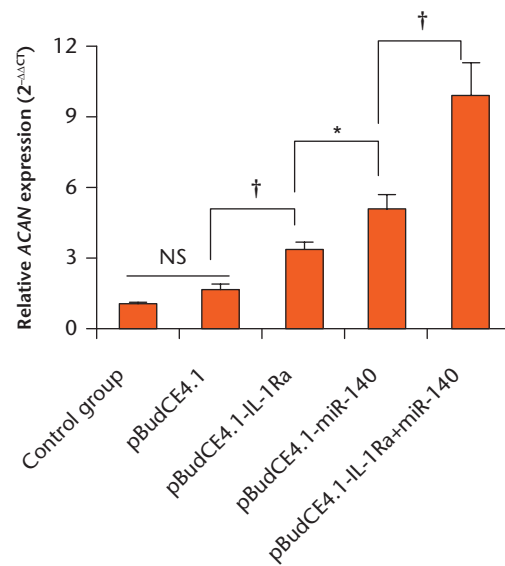


Fig. 4b

Fig. 4 (Continued)

In vivo: synovial fluid IL-1Ra, GAG, and NO concentrations. Compared with the sham group, the pBudCE4.1-IL-1Ra and pBudCE4.1-IL-1Ra+miR-140 groups presented with similar, significantly increased IL-1Ra levels (all $p < 0.01$). In the pBudCE4.1 and pBudCE4.1-miR-140 groups, IL-1Ra expression levels were not different from those of the sham group ($p > 0.05$) (Fig. 5a).

As shown in Figures 5b and 5c, compared with the sham group, all surgical groups presented with increased GAG and NO levels. The GAG and NO contents significantly decreased in the pBudCE4.1-IL-1Ra+miR-140 group, followed by the pBudCE4.1-IL-1Ra and pBudCE4.1-miR-140 groups, compared with the pBudCE4.1 group ($p < 0.05$).

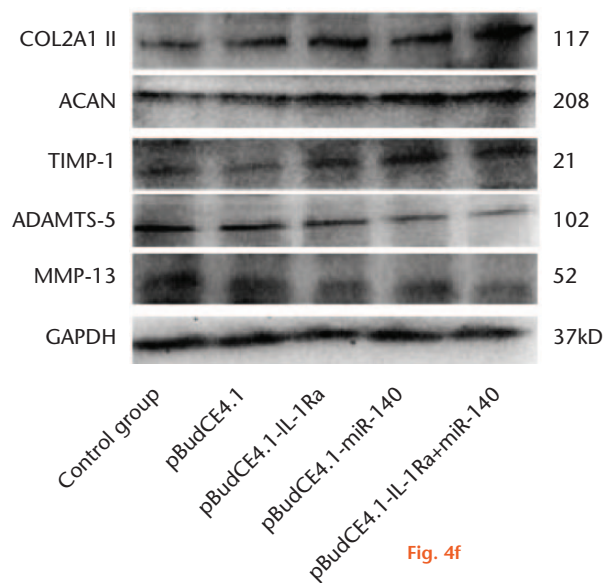
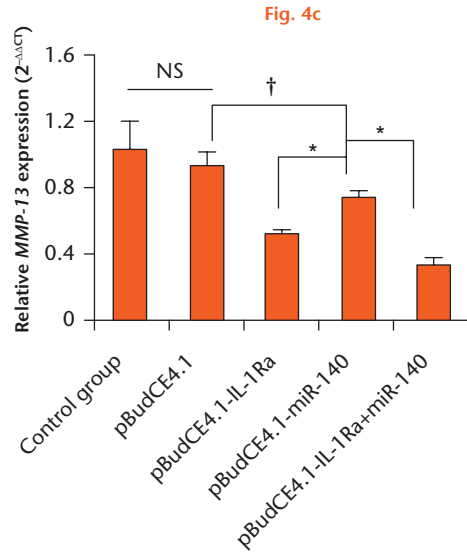
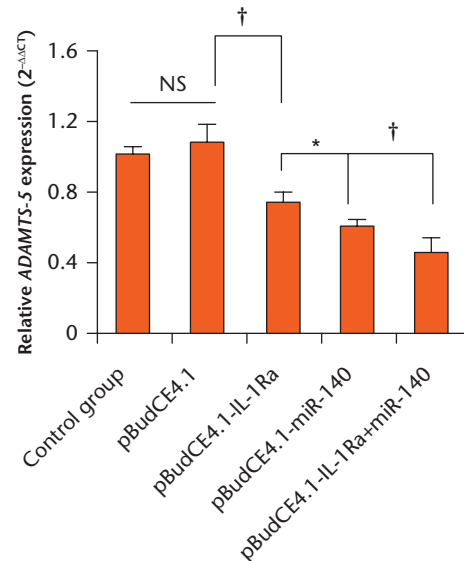
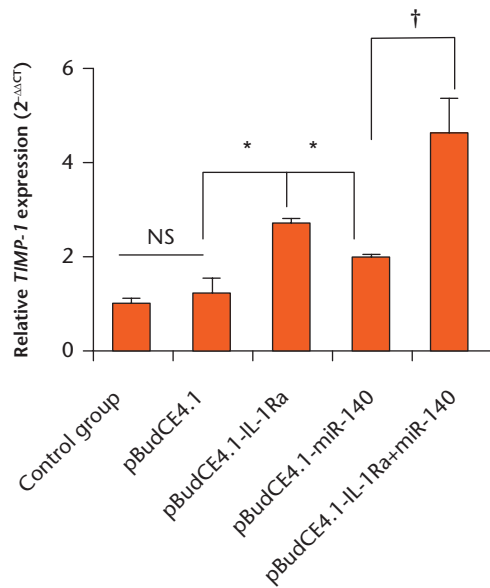


Fig. 4e

Fig. 4d

Fig. 4f

The effect of gene delivery on collagen type II alpha 1 chain (COL2A1), aggrecan (ACAN), TIMP metalloproteinase inhibitor 1 (TIMP-1), a disintegrin and metalloproteinase with thrombospondin motifs 5 (ADAMTS-5), and metalloproteinase (MMP)-13 expression in chondrocytes. Graphs showing real-time fluorescent quantitative polymerase chain reaction (RT-qPCR) assays for the mRNA expression of: a) COL2A1; b) ACAN; c) TIMP-1; d) ADAMTS-5; and e) MMP-13. The data are shown as mean values and standard deviations. The raw mRNA gene expression data for each group were calibrated to the reference gene β -2-microglobulin (B2M), and the relative expression level of each gene is represented as $2^{-\Delta\Delta CT}$. * $p < 0.05$; † $p < 0.01$; NS, not significant. f) Western blot assays for the protein expression of collagen II, aggrecan, TIMP-1, ADAMTS-5, and MMP-13. Glyceraldehyde 3-phosphate dehydrogenase (GAPDH) was used as the internal control.

In vivo: quantitative miR-140, COL2A1, ACAN, TIMP-1, ADAMTS-5, and MMP-13 expression in cartilage. The miR-140 expression levels in cartilage were similarly increased in the pBudCE4.1-miR-140 and pBudCE4.1-IL-1Ra+miR-140 groups compared with the other groups ($p < 0.001$). No significant differences were observed between the pBudCE4.1-IL-1Ra and sham groups ($p = 0.608$) or between the pBudCE4.1 and sham groups ($p = 0.829$) (Fig. 6a). Compared with the sham group, the pBudCE4.1-IL-1Ra+miR-140, pBudCE4.1-miR-140, and

pBudCE4.1-IL-1Ra groups presented with significantly upregulated expression levels of COL2A1, ACAN, and TIMP-1 ($p < 0.05$). No significant difference in the expression of these genes was detected between the control and pBudCE4.1 groups ($p > 0.05$) (Figs 6b to 6d).

Compared with the sham group, the surgical group presented with significantly upregulated expression levels of ADAMTS-5 and MMP-13. Compared with the pBudCE4.1 group, the pBudCE4.1-IL-1Ra+miR-140, pBudCE4.1-miR-140, and pBudCE4.1-IL-1Ra groups

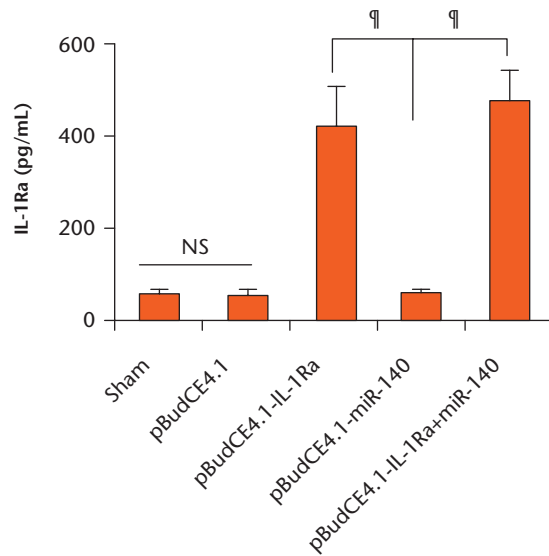


Fig. 5a

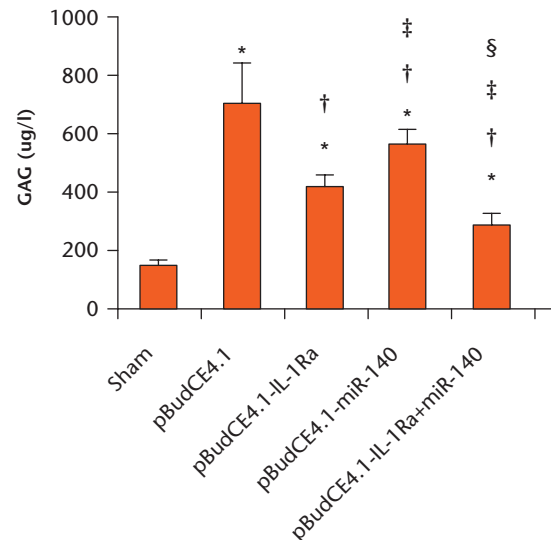


Fig. 5b

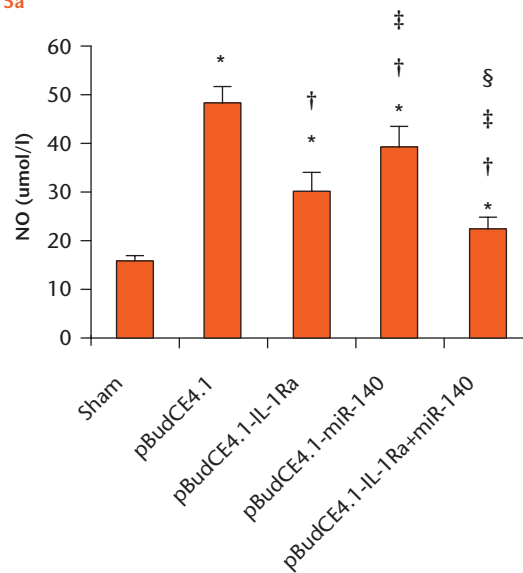


Fig. 5c

Graphs showing synovial fluid concentrations of: a) interleukin-1 receptor antagonist protein (IL-1Ra); b) glycosaminoglycan (GAG); and c) nitric oxide (NO). The concentration of IL-1Ra and GAG was determined by enzyme-linked immunosorbent assay (ELISA). The NO concentration was measured by a nitrate reductase assay. The data are shown as mean values and standard deviations. * $p < 0.05$ versus control group; † $p < 0.05$ versus pBudCE4.1; ‡ $p < 0.05$ versus pBudCE4.1-IL-1Ra; § $p < 0.05$ versus pBudCE4.1-miR-140; NS, not significant.

presented with significantly downregulated expression levels of ADAMTS-5 and MMP-13 (all $p < 0.05$) (Figs 6e and 6f). Moreover, the COL2A1, ACAN, and MMP-13 mRNA expression levels were higher in the pBudCE4.1-miR-140 group than in the pBudCE4.1-IL-1Ra group (all $p < 0.05$) (Figs 6b, 6c, and 6f). The TIMP-1 and ADAMTS-5 mRNA expression levels were lower in the pBudCE4.1-miR-140 group than in the pBudCE4.1-IL-1Ra group (all $p < 0.05$) (Figs 6d and 6e).

Histological examination of articular cartilage: H&E staining. The articular cartilage surface was generally smooth and continuous, the ECM was uniformly stained, and the laminar structure was clear in the sham group. In

the pBudCE4.1 group, the defect was partially filled with inflammatory cells and fibrous tissue, and different levels of cartilage repair appeared in the pBudCE4.1-IL-1Ra, pBudCE4.1-miR-140, and pBudCE4.1-IL-1Ra+miR-140 groups. The most complete repair appeared in the pBudCE4.1-IL-1Ra+miR-140 group, which was almost completely filled with nascent cartilage (Fig. 7a).

Histological examination of articular cartilage: safranin O/fast green staining. In the sham group, normal uniform safranin O/fast green staining and structural organization was observed, but safranin O staining was negative in the defect area of the pBudCE4.1 group. Different safranin O staining intensities appeared in the defect

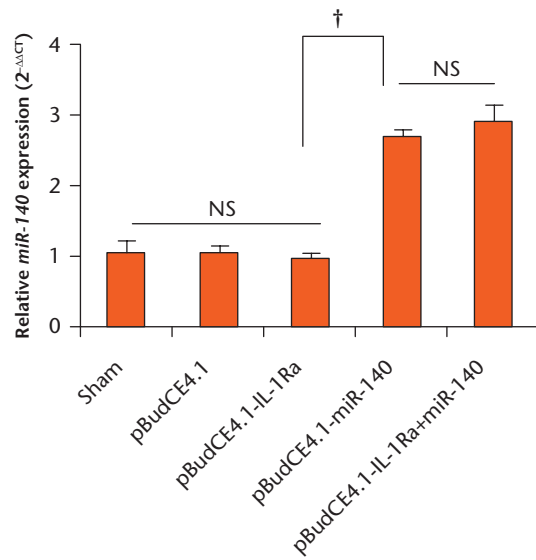


Fig. 6a

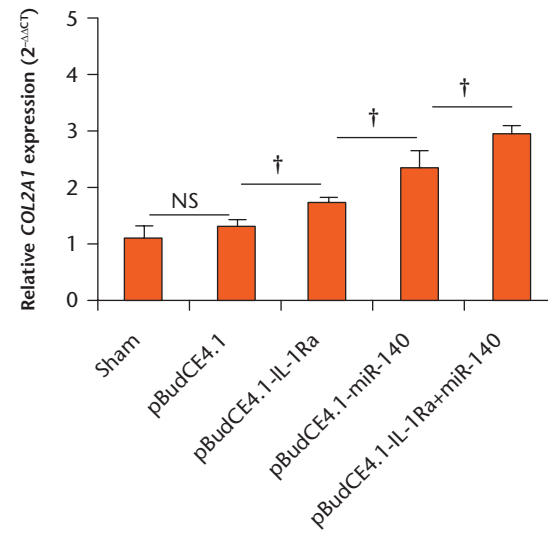


Fig. 6b

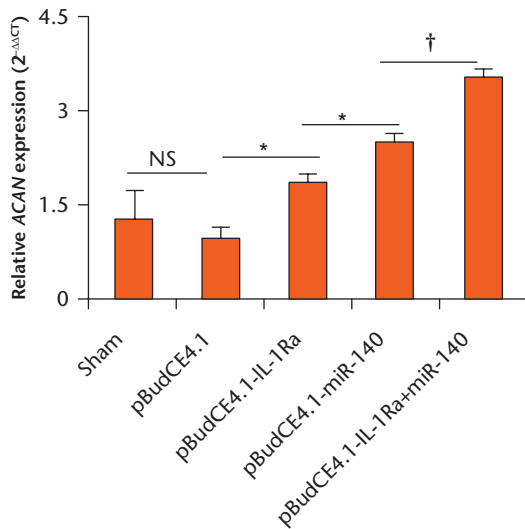


Fig. 6c

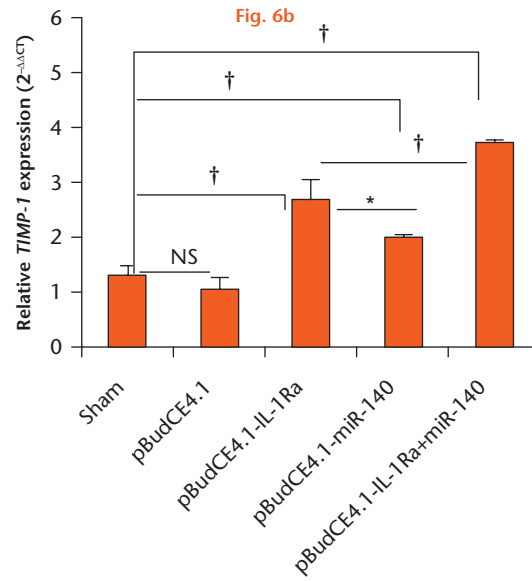


Fig. 6d

Fig. 6 (Continued)

area of the pBudCE4.1-IL-1Ra, pBudCE4.1-miR-140, and pBudCE4.1-IL-1Ra+miR-140 groups (Fig. 7b). Mankin scores are shown in Table II.

Histological examination of articular cartilage: immunohistochemistry. Chondrocytes were observed in the middle of the main layer of the sham group and were found to contain a large amount of COL2A1 and ACAN protein, staining dark brown in the ECM. In the defect area of the pBudCE4.1 group, inflammatory cells and fibrous tissue produced a slight, non-specific colouration. In the defect area of the pBudCE4.1-IL-1Ra, pBudCE4.1-miR-140, and pBudCE4.1-IL-1Ra+miR-140 groups, a large amount of COL2A1 and ACAN protein was detected in the ECM of the new cartilage. Chondrocyte morphology and

colouration in the pBudCE4.1-IL-1Ra+miR-140 group was close to that of the sham group (Figs 7c and 7d).

Discussion

CS can crosslink with collagen macromolecules.^{30,31} When cartilage is damaged, chondrocytes and collagen are exposed, which facilitates CS nanoparticle localization and the expression of exogenous genes in the defect, resulting in a therapeutic effect. Our previous studies used pNNS-CS as a gene carrier (with the pNNS containing an SV40 nuclear localization signal and a potentially phosphorylatable serine residue), and *in vitro* experiments have confirmed that pNNS-CS can transport pDNA into the nucleus and intensively augment exogenous

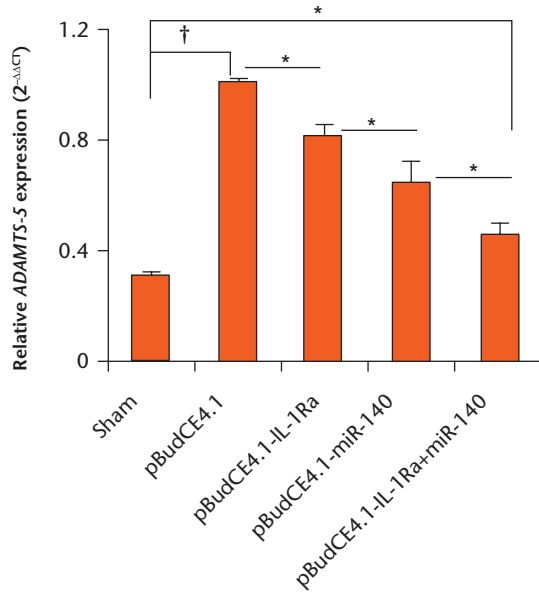


Fig. 6e

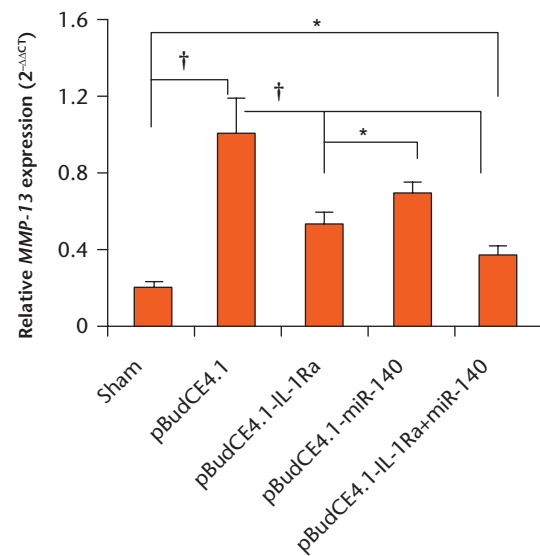


Fig. 6f

Graphs showing relative gene expression in cartilage assessed by real-time fluorescent quantitative polymerase chain reaction (RT-qPCR) for: a) miR-140; b) collagen type II alpha 1 chain (COL2A1); c) aggrecan (ACAN); d) TIMP metalloproteinase inhibitor 1 (TIMP-1); e) a disintegrin and metalloproteinase with thrombospondin motifs 5 (ADAMTS-5); and f) metalloproteinase (MMP)-13. The raw expression data for miR-140, COL2A1, ACAN, TIMP-1, ADAMTS-5, and MMP-13 for each group were calibrated to the U6 or β -2-microglobulin (B2M) reference gene, and the relative expression level of each gene is represented as $2^{-\Delta\Delta CT}$. The miR-140, COL2A1, ACAN, TIMP-1, ADAMTS-5, and MMP-13 expression levels were normalized to the expression of the control group, in which the gene expression levels were arbitrarily set to 1.0. The data are shown as mean values and standard deviations. * $p < 0.05$; † $p < 0.01$; NS, not significant.

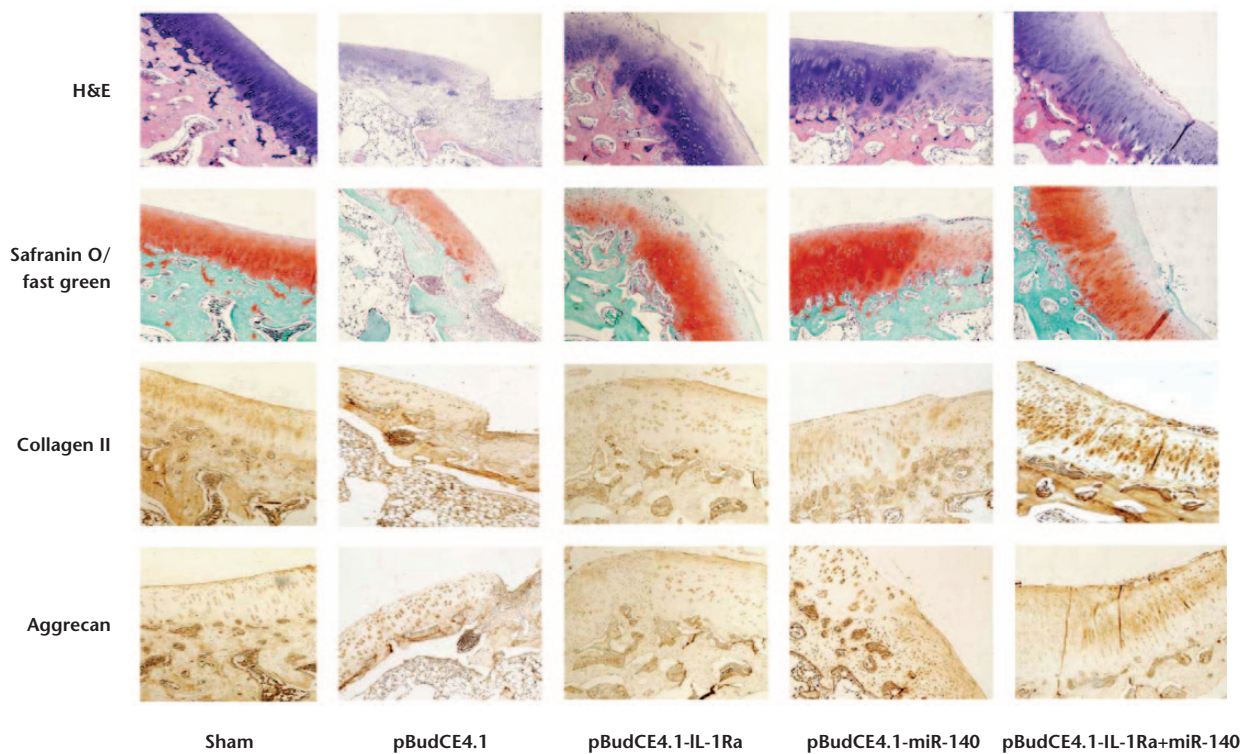


Fig. 7

Histological analysis of changes in rabbit articular cartilage. Eight weeks after surgery, the rabbits were sacrificed, and the sagittal medial femoral condyles of knee were stained with haematoxylin and eosin (H&E), safranin O/fast green, collagen II, and aggrecan. The data shown are representative microscopic images of rabbit knees from each group (original magnification 40 \times).

Table II. Mankin scores of articular cartilage specimens in each group

Group	Rabbits, n	Mean (sd)*
Sham	6	0.50 (0.55)
pBudCE4.1	6	10.83 (1.72)
pBudCE4.1-IL-1Ra	6	7.67 (0.82)
pBudCE4.1-miR-140	6	6.17 (1.33)
pBudCE4.1-IL-1Ra+miR-140	6	3.67 (1.03)

*Mankin scores of articular cartilage specimens from each group compared with p < 0.05.

gene expression, which is mainly related to the fact that pNNS can assist the nuclear localization and intra-nuclear disassociation of exogenes.¹³ The results encourage us to use pNNS-CS to mediate gene transfection in chondrocytes. Here, we investigated the use of pNNS-CS-mediated gene transfection in chondrocytes to promote efficient expression both *in vitro* and *in vivo*, as well as its effects on cartilage defect repair. In this study, we first verified that pNNS-CS can improve transfection efficiency in chondrocytes. Second, the results demonstrated that pNNS-CS-mediated pBudCE4.1-IL-1Ra, pBudCE4.1-miR-140, or pBudCE4.1-IL-1Ra+miR-140 gene transfection in chondrocytes can induce IL-1Ra and miR-140 overexpression both *in vitro* and *in vivo*.

Many miRNAs play critical roles in cartilage-specific processes.³²⁻³⁵ miR-140 inhibits cartilage ECM degradation by inhibiting MMP-13 and ADAMTS-5 expression.^{17,36,37} miR-140 expression in cartilage is reduced during osteoarthritis, and the inflammatory signalling associated with cartilage degradation inhibits miR-140 expression.^{37,38} miR-140^{-/-} mice present with age-related osteoarthritis-like changes.³⁹ Many studies have tried to use miR-140 to interfere with cartilage-related diseases.^{22,24,36,38} IL-1Ra can block IL-1 binding the IL-1 receptor, which is associated with cartilage damage and prevents damaged cartilage repair.⁴⁰ In human patients, cartilage injuries are often accompanied by a significant decrease in IL-1Ra levels.⁴¹ IL-1Ra gene transfer promoted cartilage defect repair in a rabbit model.^{10,15} IL-1Ra protein treatment prevented injury-induced cartilage matrix degradation and increased miR-140 expression in cartilage.²⁶ IL-1 β repressed miR-140 expression in cartilage.^{24,42} Considering the roles of IL-1Ra and miR-140 in chondrocytes and the relationship between these two molecules, we proposed that IL-1Ra and miR-140 might be synergistic in promoting cartilage defect repair. Our experimental results reveal that IL-1Ra and miR-140 introduction by pNNS-CS transfection have a positive effect both *in vitro* and *in vivo*, and the effects of this two-gene combination are better than those of a single gene.

IL-1 β stimulates chondrocytes to release the catabolic factor NO. NO can induce MMP synthesis and inhibit collagen and proteoglycan synthesis in chondrocytes, and high NO concentrations significantly inhibit chondrocyte proliferation and induce chondrocyte apoptosis.^{43,44} NO

is considered to be closely related to cartilage damage. In this study, the results revealed that IL-1Ra and miR-140 overexpression inhibits NO production and protects chondrocytes against the anti-proliferation effect of IL-1 β , and this two-gene combination significantly enhanced these effects both *in vitro* and *in vivo*.

The cartilage ECM components mainly include COL2A1, ACAN, and GAGs. *In vitro*, chondrocyte redifferentiation was supported by COL2A1, ACAN, and GAG biosynthesis.⁴⁵ Changes in the COL2A1, ACAN, and GAG levels therefore reflect the anabolic level of the cartilage ECM.⁴⁶ In this study, compared with the control group, the groups with IL-1Ra and miR-140 overexpression each individually presented with increased GAG accumulation in the cell supernatants and COL2A1 and ACAN expression in the chondrocyte, and the joint IL-1Ra and miR-140 treatment significantly enhanced these effects. When cartilage is damaged *in vivo*, the damage causes GAG release into the synovial fluid. Therefore, changes in the synovial fluid GAG concentration reflect the degree of catabolic activity in the cartilage ECM.⁴⁶ In this study, compared with cartilage damage in the sham group, cartilage damage in the negative control group (pBudCE4.1 transfection group) increased the synovial fluid GAG content and decreased COL2A1 and ACAN expression in cartilage. Compared with the negative control group, the IL-1Ra- and miR-140-overexpressing groups each individually reduced the synovial fluid GAG content and increased COL2A1 and ACAN expression, and a lower synovial fluid GAG content and higher COL2A1 and ACAN expression were detected in the joint IL-1Ra and miR-140 group. These effects are particularly important during articular cartilage repair because these changes imply that the repair tissue filling the cartilage lesion possesses similar characteristics to hyaline cartilage. The increased GAG, COL2A1, and ACAN expression suggests that IL-1Ra and miR-140 have cartilage repair functions.

TIMP-1 inhibits the role of MMPs, promotes cell proliferation, and reduces cell apoptosis.²² Thus, in this study, the IL-1Ra and miR-140-induced TIMP-1 upregulation may explain the ECM production and chondrocyte proliferation. ADAMTS-5 and MMP-13 were involved in the progressive erosion of articular cartilage. IL-1Ra^{26,47} and miR-140^{17,22,37} significantly reduce ADAMTS-5 and MMP-13 expression, and increase the TIMP-1 level, thus inhibiting ECM proteoglycan and collagen degradation. In this study, IL-1Ra and miR-140 each individually induced beneficial effects on ADAMTS-5, MMP-13, and TIMP-1 levels. These findings are consistent with the results of previous studies.^{17,22,26,37,47} The most beneficial effects were detected in the joint IL-1Ra and miR-140 group. Histological analysis also showed that IL-1Ra and miR-140 significantly lowered the Mankin score of the cartilage defect and promoted COL2A1 and ACAN synthesis in the ECM. Based on the *in vitro* GAG findings, the

safranin O/fast green staining results indicated that IL-1Ra and miR-140 increased proteoglycan synthesis. All the results strongly suggest that the synergistic effects of IL-1Ra and miR-140 were clearly superior to the effects of IL-1Ra or miR-140 alone, not only for promoting cartilage proliferation, but also for inhibiting the inflammatory response and cartilage degradation.

In conclusion, our findings show that pNNS-CS complexes can efficiently carry exogenous genes into rabbit chondrocytes and promote expression both *in vitro* and *in vivo*. Our study also provided direct experimental evidence for the synergistic effect of IL-1Ra and miR-140 on repairing cartilage defects by enhancing chondrocyte proliferation, proteoglycan synthesis, and COL2A1 and ACAN expression. Meanwhile, the combination of these two exogenous genes has better biological effects than either IL-1Ra or miR-140 alone. Further work is necessary to study pNNS-CS transfection efficiency in cells from other species, including human chondrocytes, and the synergistic mechanisms of selected genes in cartilage defects.

References

1. Simental-Mendía M, Lara-Arias J, Álvarez-Lozano E, et al. Cotransfected human chondrocytes: over-expression of IGF-I and SOX9 enhances the synthesis of cartilage matrix components collagen-II and glycosaminoglycans. *Braz J Med Biol Res* 2015;48:1063-1070.
2. Hemphill DD, McIlwraith CW, Slayden RA, Samulski RJ, Goodrich LR. Adeno-associated virus gene therapy vector scAAVIGF-I for transduction of equine articular chondrocytes and RNA-seq analysis. *Osteoarthritis Cartilage* 2016;24:902-911.
3. Cucchiariini M, Madry H. Overexpression of human IGF-I via direct rAAV-mediated gene transfer improves the early repair of articular cartilage defects in vivo. *Gene Ther* 2014;21:811-819.
4. Shi S, Mercer S, Eckert GJ, Trippel SB. Growth factor transgenes interactively regulate articular chondrocytes. *J Cell Biochem* 2013;114:908-919.
5. Tao K, Rey-Rico A, Frisch J, et al. rAAV-mediated combined gene transfer and overexpression of TGF- β and SOX9 remodels human osteoarthritic articular cartilage. *J Orthop Res* 2016;34:2181-2190.
6. Oliveira AV, Silva GA, Chung DC. Enhancement of chitosan-mediated gene delivery through combination with phiC31 integrase. *Acta Biomater* 2015;17:89-97.
7. Wang Z, Wu G, Wei M, et al. Improving the osteogenesis of human bone marrow mesenchymal stem cell sheets by microRNA-21-loaded chitosan/hyaluronic acid nanoparticles via reverse transfection. *Int J Nanomedicine* 2016;11:2091-2105.
8. Veilleux D, Gopalakrishna Panicker RK, Chevrier A, et al. Lyophilisation and concentration of chitosan/siRNA polyplexes: influence of buffer composition, oligonucleotide sequence, and hyaluronic acid coating. *J Colloid Interface Sci* 2018;512:335-345.
9. Tezgel Ö, Szarpak-Jankowska A, Arnould A, Auzély-Velty R, Texier I. Chitosan-lipid nanoparticles (CS-LNPs): application to siRNA delivery. *J Colloid Interface Sci* 2018;510:45-56.
10. Zhao R, Peng X, Li Q, Song W. Effects of phosphorylatable short peptide-conjugated chitosan-mediated IL-1Ra and igf-1 gene transfer on articular cartilage defects in rabbits. *PLoS One* 2014;9:e112284.
11. Xiong Q, Chen J, Li FL, et al. Co-expression of mFat-1 and pig IGF-1 genes by recombinant plasmids in modified chitosan nanoparticles and its synergistic effect on mouse immunity. *Sci Rep* 2017;7:17136.
12. Baghdan E, Pinnareddy SR, Strehlow B, et al. Lipid coated chitosan-DNA nanoparticles for enhanced gene delivery. *Int J Pharm* 2018;535:473-479.
13. Zhao R, Sun B, Liu T, et al. Optimize nuclear localization and intra-nucleus disassociation of the exogene for facilitating transfection efficacy of the chitosan. *Int J Pharm* 2011;413:254-259.
14. Frisch J, Rey-Rico A, Venkatesan JK, et al. rAAV-mediated overexpression of sox9, TGF- β and IGF-I in minipig bone marrow aspirates to enhance the chondrogenic processes for cartilage repair. *Gene Ther* 2016;23:247-255.
15. Zhang P, Zhong ZH, Yu HT, Liu B. Exogenous expression of IL-1Ra and TGF- β 1 promotes *in vivo* repair in experimental rabbit osteoarthritis. *Scand J Rheumatol* 2015;44:404-411.
16. Armbruster N, Krieg J, Weibenberger M, Scheller C, Steinert AF. Rescued chondrogenesis of mesenchymal stem cells under interleukin 1 challenge by foamyviral interleukin 1 receptor antagonist gene transfer. *Front Pharmacol* 2017;8:255.
17. Gibson G, Asahara H. microRNAs and cartilage. *J Orthop Res* 2013;31:1333-1344.
18. Diaz-Prado S, Cicione C, Muiños-López E, et al. Characterization of microRNA expression profiles in normal and osteoarthritic human chondrocytes. *BMC Musculoskelet Disord* 2012;13:144.
19. Ntoumou E, Tzetis M, Braoudaki M, et al. Serum microRNA array analysis identifies miR-140-3p, miR-33b-3p and miR-671-3p as potential osteoarthritis biomarkers involved in metabolic processes. *Clin Epigenetics* 2017;9:127.
20. Yin CM, Suen WC, Lin S, et al. Dysregulation of both miR-140-3p and miR-140-5p in synovial fluid correlate with osteoarthritis severity. *Bone Joint Res* 2017;6:612-618.
21. Trzeciak T, Czarny-Ratajczak M. MicroRNAs: important epigenetic regulators in osteoarthritis. *Curr Genomics* 2014;15:481-484.
22. Li X, Zhen Z, Tang G, Zheng C, Yang G. miR-29a and miR-140 protect chondrocytes against the anti-proliferation and cell matrix signaling changes by IL-1 β . *Mol Cells* 2016;39:103-110.
23. Vonk LA, Kragten AH, Dhert WJ, Saris DB, Creemers LB. Overexpression of hsa-miR-148a promotes cartilage production and inhibits cartilage degradation by osteoarthritic chondrocytes. *Osteoarthritis Cartilage* 2014;22:145-153.
24. Tao SC, Yuan T, Zhang YL, et al. Exosomes derived from miR-140-5p-overexpressing human synovial mesenchymal stem cells enhance cartilage tissue regeneration and prevent osteoarthritis of the knee in a rat model. *Theranostics* 2017;7:180-195.
25. Zhang R, Ma J, Yao J. Molecular mechanisms of the cartilage-specific microRNA-140 in osteoarthritis. *Inflamm Res* 2013;62:871-877.
26. Genemaras AA, Reiner T, Huang CY, Kaplan L. Early intervention with interleukin-1 receptor antagonist protein modulates catabolic microRNA and mRNA expression in cartilage after impact injury. *Osteoarthritis Cartilage* 2015;23:2036-2044.
27. Cheng W, Wu D, Zuo Q, Wang Z, Fan W. Ginsenoside Rb1 prevents interleukin-1 beta induced inflammation and apoptosis in human articular chondrocytes. *Int Orthop* 2013;37:2065-2070.
28. Peng XX, Zhao RL, Song W, et al. Selection of suitable reference genes for normalization of quantitative real-time PCR in cartilage tissue injury and repair in rabbits. *Int J Mol Sci* 2012;13:14344-14355.
29. Mankin HJ, Dorfman H, Lippiello L, Zarins A. Biochemical and metabolic abnormalities in articular cartilage from osteo-arthritic human hips. II. Correlation of morphology with biochemical and metabolic data. *J Bone Joint Surg [Am]* 1971;53-A:523-537.
30. Kaczmarek B, Sionkowska A, Osyczka AM. The application of chitosan/collagen/hyaluronic acid sponge cross-linked by dialdehyde starch addition as a matrix for calcium phosphate *in situ* precipitation. *Int J Biol Macromol* 2018;107:470-477.
31. Wang X, Wang G, Liu L, Zhang D. The mechanism of a chitosan-collagen composite film used as biomaterial support for MC3T3-E1 cell differentiation. *Sci Rep* 2016;6:39322.
32. Yu CD, Miao WH, Zhang YY, Zou MJ, Yan XF. Inhibition of miR-126 protects chondrocytes from IL-1 β induced inflammation via upregulation of Bcl-2. *Bone Joint Res* 2018;7:414-421.
33. Jin Y, Chen X, Gao ZY, et al. The role of miR-320a and IL-1 β in human chondrocyte degradation. *Bone Joint Res* 2017;6:196-203.
34. Hu J, Wang Z, Pan Y, et al. miR-26a and miR-26b mediate osteoarthritis progression by targeting FUT4 via NF- κ B signaling pathway. *Int J Biochem Cell Biol* 2018;94:79-88.
35. Xu J, Lv S, Hou Y, et al. miR-27b promotes type II collagen expression by targeting peroxisome proliferator-activated receptor- γ 2 during rat articular chondrocyte differentiation. *Biosci Rep* 2018;38:BSR20171109.
36. Si HB, Zeng Y, Liu SY, et al. Intra-articular injection of microRNA-140 (miRNA-140) alleviates osteoarthritis (OA) progression by modulating extracellular matrix (ECM) homeostasis in rats. *Osteoarthritis Cartilage* 2017;25:1698-1707.
37. Proctor CJ, Smith GR. Computer simulation models as a tool to investigate the role of microRNAs in osteoarthritis. *PLoS One* 2017;12:e0187568.
38. Si H, Zeng Y, Zhou Z, et al. Expression of miRNA-140 in chondrocytes and synovial fluid of knee joints in patients with osteoarthritis. *Chin Med Sci J* 2016;31:207-212.
39. Miyaki S, Sato T, Inoue A, et al. MicroRNA-140 plays dual roles in both cartilage development and homeostasis. *Genes Dev* 2010;24:1173-1185.

40. Calich AL, Domiciano DS, Fuller R. Osteoarthritis: can anti-cytokine therapy play a role in treatment? *Clin Rheumatol* 2010;29:451-455.
41. Bigoni M, Sacerdote P, Turati M, et al. Acute and late changes in intraarticular cytokine levels following anterior cruciate ligament injury. *J Orthop Res* 2013;31:315-321.
42. Liang Y, Duan L, Xiong J, et al. E2 regulates MMP-13 via targeting miR-140 in IL-1 β -induced extracellular matrix degradation in human chondrocytes. *Arthritis Res Ther* 2016;18:105.
43. Zheng W, Feng Z, Lou Y, et al. Silibinin protects against osteoarthritis through inhibiting the inflammatory response and cartilage matrix degradation in vitro and in vivo. *Oncotarget* 2017;8:99649-99665.
44. de Andrés MC, Takahashi A, Oreffo RO. Demethylation of an NF- κ B enhancer element orchestrates iNOS induction in osteoarthritis and is associated with altered chondrocyte cell cycle. *Osteoarthritis Cartilage* 2016;24:1951-1960.
45. Payr S, Tichy B, Atteneo C, et al. Redifferentiation of aged human articular chondrocytes by combining bone morphogenetic protein-2 and melanoma inhibitory activity protein in 3D-culture. *PLoS One* 2017;12:e0179729.
46. Tsuchida AI, Beekhuizen M, Rutgers M, et al. Interleukin-6 is elevated in synovial fluid of patients with focal cartilage defects and stimulates cartilage matrix production in an in vitro regeneration model. *Arthritis Res Ther* 2012;14:R262.
47. Chen B, Qin J, Wang H, Magdalou J, Chen L. Effects of adenovirus-mediated bFGF, IL-1Ra and IGF-1 gene transfer on human osteoarthritic chondrocytes and osteoarthritis in rabbits. *Exp Mol Med* 2010;42:684-695.

Author contributions

- R. Zhao: Designed the study, Performed the experiments, Analyzed the results, Wrote the manuscript.
- S. Wang: Performed the experiments.
- L. Jia: Performed the experiments.
- Q. Li: Performed the experiments.
- J. Qiao: Performed the experiments.
- X. Peng: Designed the study, Performed the experiments, Analyzed the results, Wrote the manuscript.

Funding statement

- This work was supported by the National Natural Science Foundation of China (No. 81770915, 81301737); the Shandong Provincial Natural Science Foundation, China (No. ZR2012HQ034, ZR2015HL025); and the PhD program of Weifang Medical University, China (No. 2017BSQD05).
- No benefits in any form have been received or will be received from a commercial party related directly or indirectly to the subject of this article.

Ethical review statement

- The protocols in this study that involved animals were approved by the Institutional Animal Care and Use Committee of Weifang Medical University.

© 2019 Author(s) et al. This is an open-access article distributed under the terms of the Creative Commons Attribution licence (CC-BY-NC), which permits unrestricted use, distribution, and reproduction in any medium, but not for commercial gain, provided the original author and source are credited.